The Cryosphere Discuss., 9, 4437–4457, 2015
www.the-cryosphere-discuss.net/9/4437/2015/
doi:10.5194/tcd-9-4437-2015

The Cryosphere Discussions
Open Access

The electrical self-potential method is a non-intrusive snow-hydrological sensor

S. S. Thompson[1,a], **B. Kulessa**[2], **R. L. H. Essery**[3], **and M. P. Lüthi**[4,a]

[1]Department of Arctic Geology, University Centre in Svalbard (UNIS), Svalbard, Norway
[2]College of Science, Swansea University, Swansea, UK
[3]The School of Geosciences, University of Edinburgh, Edinburgh, UK
[4]University of Zurich, Zurich, Switzerland
[a]formerly at: Versuchsanstalt für Wasserbau, Hydrologie und Glaziologie (VAW), ETH Zürich, Zurich, Switzerland

Received: 8 July 2015 – Accepted: 29 July 2015 – Published: 24 August 2015

Correspondence to: S. S. Thompson (sarah.thompson@unis.no)

Published by Copernicus Publications on behalf of the European Geosciences Union.

Abstract

Our ability to measure, quantify and assimilate hydrological properties and processes of snow in operational models is disproportionally poor compared to the significance of seasonal snowmelt as a global water resource and major risk factor in flood and avalanche forecasting. Encouraged by recent theoretical, modelling and laboratory work, we show here that the diurnal evolution of aerially-distributed self-potential magnitudes closely track those of bulk meltwater fluxes in melting in-situ snowpacks at Rhone and Jungfraujoch glaciers, Switzerland. Numerical modelling infers temporally-evolving liquid water contents in the snowpacks on successive days in close agreement with snow-pit measurements. Muting previous concerns, the governing physical and chemical properties of snow and meltwater became temporally invariant for modelling purposes. Because measurement procedure is straightforward and readily automated for continuous monitoring over significant spatial scales, we conclude that the self-potential geophysical method is a highly-promising non-intrusive snow-hydrological sensor for measurement practice, modelling and operational snow forecasting.

1 Introduction

More than a sixth of the world's population relies on melt from seasonal snow and glaciers for water supply (Barnett et al., 2005). Snow, and runoff from snow, are also major resources for the hydroelectric, tourism and inland fishery industries, and furthermore represent hazards from flooding and avalanches (Mitterer et al., 2011). The availability of snow models constrained by a reliable observational basis, for the forecasting of snow hydrological properties and processes in climate, resource and hazard applications is therefore of considerable socio-economic significance (Wever et al., 2014). However, the parameterisation of fundamental snow-hydrological attributes, such as liquid water content and flux, is a well-recognised major source of uncertainty in operational models used in snow and hydrological forecasting (Livneh et al., 2010; Es-

sery et al., 2013). Uncertainty is rooted principally in the inability of traditional snow-hydrological techniques to provide automated attribute measurements non-invasively and on spatial scales that match those used in operational snow models. Relevant traditional techniques include dielectric (Denoth, 1994) or "hand" tests (Fierz et al., 2009) of snow liquid water contents, lysimeter measurements of discharge, temperature and pH and electrical conductivity of bulk meltwaters (Campbell et al., 2006; Williams et al., 2010), and manual observation or measurement of snow density and grain size (Fierz et al., 2009).

By combining field measurements with numerical modelling we show here that a combination of traditional with electrical self-potential geophysical measurements can address these limitations. The self-potential technique is a passive geo-electrical method that exploits the presence of naturally-occurring electrical potentials in the subsurface generated when water flows through a porous matrix ("streaming potential"; Darnet et al., 2003; Revil et al., 2006). The technique is well established for a number of subsurface hydrological problems, including aquifer characterization, mapping pollutant plumes and monitoring seepage in earth dams (Revil et al., 2003; Sheffer and Oldenburg, 2007; Doherty et al., 2010). A new theory and numerical model of self-potential signals associated with unsaturated flow in melting snow, along with laboratory tests, strongly promoted the technique as a non-intrusive hydrological sensor of water fluxes (Kulessa et al., 2012); at spatial scales intermediate between snow pits and satellite footprints or, given independent flux measurements, of evolving physical and chemical properties of snow and snow-melt.

We answer three fundamental questions: (1) can the self-potential method serve as a non-intrusive sensor of snow hydrological properties and processes? (2) How sensitive are retrievals of liquid water content from self-potential to snow physical and chemical properties? (3) What are the hydrological implications for future snow measurement and modelling research and practice? Our study thus takes a significant step towards the in-situ implementation of the self-potential method for improved characterization and monitoring of snow liquid water contents and melt water fluxes.

2 Model, field sites and methods

The Poisson equation relates the electrical field ψ to the source current density in a partially or fully-saturated snow pack,

$$\nabla \cdot (\sigma \nabla \psi) = \nabla \cdot \boldsymbol{j}_{\mathrm{S}}, \tag{1}$$

where σ is the bulk electrical conductivity of the porous material (in $\mathrm{S\,m^{-1}}$), and $\boldsymbol{j}_{\mathrm{S}}$ is the source current density (in $\mathrm{A\,m^{-2}}$) (Kulessa et al., 2012). Equation (1) applies only in the low-frequency limit of the Maxwell's equations without external injection or retrieval of charges, or charge storage in the snowpack. Extending the classic Helmholtz–Smoluchowski theory for unsaturated flow in snow, the one-dimensional solution to Eq. (1) is given by

$$\psi_{\mathrm{m}} - \psi_0 = -\frac{\varepsilon \zeta}{\eta \sigma_{\mathrm{w}}} S_{\mathrm{w}} (H_{\mathrm{m}} - H_0), \tag{2}$$

where ψ_{m} and H_{m} are respectively the electrical and hydraulic potentials at the measurement electrode, ψ_0 and H_0 are the corresponding potentials at the reference electrode, ζ is the zeta potential (V), and ε, η, σ_{w} and S_{w} are respectively the dielectric permittivity ($\mathrm{F\,m^{-1}}$), electrical conductivity ($\mathrm{S\,m^{-1}}$), dynamic viscosity (in Pa s) and relative saturation (dimensionless) of the melt or rainwaters in the snowpack's pore space (Kulessa et al., 2012). The zeta potential is the voltage across the electrical double layer at the interface between the ice matrix and the pore waters, as controlled by these constituents' physical and electrical properties. If ψ_0 and H_0 have negligible magnitudes compared to the self-potential field ψ, the relationship between ψ and bulk discharge Q ($\mathrm{m^3\,s^{-1}}$) in the snow pack through cross-sectional area A ($\mathrm{m^2}$) is:

$$\psi_{\mathrm{m}} = \frac{\varepsilon \zeta}{\sigma_{\mathrm{w}}} \frac{S_{\mathrm{w}}}{S_{\mathrm{e}}^{n}} \frac{1}{kA} Q, \tag{3}$$

where S_e is effective saturation and $n \approx 3.3$ is the saturation exponent (Kulessa et al., 2012).

To address the three specific objectives through data-driven testing of this model, an experimental concept was developed that simulates in-situ at two glaciers in Valais, Switzerland, the geometry of Kulessa et al. (2012) laboratory snow column and numerical model, measuring all relevant snow-hydrological attributes. Self-potential and traditional snow-hydrological measurements were acquired on 13, 14 and 15 June 2013 from the ablation area snowpack at Rhone Glacier, and 5 September 2013 from the glacial accumulation area at Jungfraujoch (Fig. 1a). At Rhone and Jungfraujoch glaciers site elevations were respectively 2340 and 3460 m a.s.l., with surface gradients of ∼ 8 and 17°. At the Rhone Glacier all three days experienced comparable air temperature, although 15 June was noticeably cloudier with a very low sunshine duration. Because daily average temperatures were between 5 and 15 °C with no fresh snowfall (*MeteoSuisse*), the snowpacks would have experienced significant melting in the weeks before the surveys. We therefore expect them to be physically mature in terms of enhanced grain size and density due to metamorphosis, and chemically mature in terms of invariant meltwater pH and electrical conductivity as preferential elution of solutes has been completed (Kulessa et al. (2012) and references therein).

At both sites more than 100 self-potential measurements were made at the snow surface, and meltwater bulk discharge, pH and electrical conductivity, and snowpack characteristics including thickness, density, grain size and liquid water content were recorded. Adopting our established acquisition procedures (Thompson et al., 2012), we conducted all self-potential surveys using a pair of lead/lead chloride "Petiau" non-polarising electrodes (Petiau, 2000). Execution followed the potential amplitude method, employing a reference electrode in a fixed location and a roving electrode moving through the survey area at 0.5 m intervals (Fig. 1b). Self-potential surveys were conducted in profiles of 25 data points perpendicular to the principal direction of water flow, where the latter was assumed to follow the gradient indicated by snow surface topography. All self-potential measurements were taken as differential readings relative

to the reference electrode, minimizing streaming, electrochemical and thermal potentials at the latter by grounding them outside the survey areas (Fig. 1a), submerged in a glass jar, open at the top and filled with water-saturated local media (Kulessa et al., 2003a). The jar was then buried upright ∼ 1 m deep to avoid exposure to surface temperature variations. Surveys were carried out with a fixed tie-in point (measured every second line) at the reference electrode, allowing for correction of the effects of electrode polarisation and drift (Doherty et al., 2010; Thompson et al., 2012).

Bulk discharge through a snowpack is preferably measured with a lysimeter (Campbell et al., 2006; Williams et al., 2010), emplaced according to Campbell et al. (2006) at the base of Rhone Glacier's snowpack, and at the limit of the diurnal melt penetration depth at Jungfraujoch (determined by daily dye tracing experiments). Snow density (by balance) and average snow grain size (crystal card and lens) were measured, at the start and end of each self-potential survey to reveal any intermittent snow metamorphism, using standardised techniques within the top and basal layers of snow pits freshly excavated at the survey sites (Fierz et al., 2009). Liquid water content was estimated using two different techniques, including the hand test (Colbeck et al., 1990; Fierz et al., 2009) in the surface and base layers of Rhone Glacier's snow pit, and the Denoth Capacitance Meter (Denoth, 1994) in the snow pit and across a 2-D grid in the surface layers (0.4 m) at Jungfraujoch, following the same survey spacing as the self-potential measurements.

3 Field measurement results

Drift-corrected self-potential magnitudes and bulk discharges increase with time through the day until decrease begins in late afternoon (Fig. 2), without a distinguishable time lag between the magnitude and discharge data (Fig. 2b). Days 1 and 2 at Rhone glacier were characterised by higher discharges and self-potential magnitudes compared to day 3, although intriguingly bulk discharge at Jungfraujoch was akin to day 3 at Rhone glacier but self-potential magnitudes were much higher than even days

1 and 2 at Rhone glacier. The pH, electrical conductivity and temperature of meltwater, recorded with each bulk discharge measurement, show no consistent temporal or spatial variation across any of the four field surveys. Electrical conductivity values generally ranged between 1×10^{-6} and 5×10^{-6} S m^{-1} without spatial or temporal consistency, while pH ranged between 6.5 and 6.9. Snow grain size remained constant at ~ 1.5 mm at Rhone Glacier and ~ 1 mm at Jungfraujoch, while snow densities ranged between 555 and 573 kg m^{-3} without spatial or temporal consistency. At Rhone Glacier the liquid water content of snow had a wetness index of 3 irrespective of measurement time or location at the surface or base of the snow pit, associated with a liquid water content range of 3–8 % vol. (Colbeck et al., 1990). At Jungfraujoch liquid water content, measured using the Denoth meter, gave profile-averaged values of 1.5 to ~ 5.0 % vol., increasing consistently throughout the survey period. These measurements and inherent uncertainties are used below for modelling purposes, sensitivity testing and error analysis.

4 Objective 1: self-potential as a snow-hydrological sensor

Both survey areas were south facing, topographically-inclined but otherwise had no visibly distinguished surface undulations, and any snow thicknesses variations were minimal. We therefore expect changes in self-potential magnitudes to be pronounced in the downslope direction, and minimal across-slope along any individual profile (Fig. 1a). Averaging all 25 self-potential data points acquired along any particular profile, a one-dimensional upslope-downslope series of self-potential magnitudes is produced for a given survey area on a given day, together with uncertainty estimates reflecting natural spatial and temporal variability along the profile (Supplement). For each profile the acquisition time of the central data point was assigned to it, and all measurements of snowpack and meltwater properties were averaged over the same time period (~ 20 min). The upslope-downslope series of average self-potential magnitudes thus emulate measurements along a strongly inclined version of the one-dimensional snow

column used in Kulessa et al. (2012) (Fig. 1b), facilitating the application of Eq. (3) to them.

This application is dependent on four key assumptions, including, (1) water flow within the survey areas' snowpacks is laminar and homogenous (where any inhomogeneities average out over the survey grids) in three dimensions, thus bounded by an impermeable layer at the base, which has a constant and equal inclination to that of the surface, providing a constant hydraulic gradient, (2) all water contributing to the measured self-potential signal within the survey area is captured by the bulk discharge measurements, thus assuming no flow across survey area boundaries, (3) contributions to the measured self-potential signal from flow below the base of the snowpack, runoff at the surface of the snowpack, and flow outside the lateral boundaries of the survey areas' snowpacks are negligible, and the integrated long-wavelength self-potential signal generated at the surface adequately captures the bulk 3-D flow, (4) all parameters controlling the self-potential magnitude (right hand side of Eq. 3) do not vary spatially across the survey areas' snowpacks, so that our ground-truth snow-pit data apply uniformly across them.

In modelling liquid water content (S_w) we must measure or estimate all of the parameters included in Eq. (3), whilst satisfying assumptions 1 to 4 above. At both Rhone Glacier and Jungfraujoch self-potential magnitude (Ψ_m), bulk discharge (Q), electrical conductivity (σ_w) and cross-sectional area (A) were measured directly, and the dielectric permittivity of water at $\sim 0\,^{\circ}$C is well known to be 7.8×10^{-9} F m^{-1}. Permeability (k) can be derived from our snow density (ρ_s) and grain size (d) measurements using Shimizu's (1970) empirical relationship

$$k = 0.077 d^2 e^{-0.0078 \rho_s} \quad (4)$$

where k is in m^2, d is in m and ρ_s in kg m^{-3}, commonly used and robust for modelling purposes (Kulessa et al., 2012). Effective saturation (S_e) and S_w are related through the irreducible water saturation S_w^{ir} by

$$S_e = \frac{S_w - S_w^{ir}}{1 - S_w^{ir}}. \quad (5)$$

In the absence of direct measurements we adopt the commonly used values of $S_w^{ir} = 0.03$ and $n \approx 3.3$ (Kulessa et al., 2012), and assume that these values are invariant in space and time at our study sites.

The zeta potential (ζ) is unknown here and poorly constrained in general. Earlier work on artificial ice samples, of fixed bulk electrical conductivity, ascertained that the zeta potential reverses sign from $\sim +0.01$ to ~ -0.02 V as equilibrium pH increases from less than 3 to greater than 8 (Drzymala et al., 1999; Kallay et al., 2003). Recent "natural snowmelt" laboratory experiments were consistent with a progressive increase of pH from 4.3 to 6.3 and a simultaneous decrease in electrical conductivity from $\sim 1 \times 10^{-1}$ to $\sim 6 \times 10^{-7}$ S m^{-1}, as the elution of ions follows a well-known sequence (Fig. 6b in Kulessa et al., 2012). Upon conclusion of the experiments, modelled rates of change of pH and electrical conductivity were minimal and the snow column mature. The zeta potential is principally a function of pH and electrical conductivity (Kulessa et al., 2012; their Eq. 18), and was inferred to change from $\sim -7.5 \times 10^{-2}$ V at the start of their natural snowmelt experiments to $+1.5 \times 10^{-2}$ V at the end, when the rate of change of the zeta potential consistently was minimal (Fig. 7a in Kulessa et al., 2012).

The final values of pH and electrical conductivity were similar to those measured at Rhone Glacier and Jungfraujoch (respectively $\sim$ 6.5–6.9 and ~ 1–5×10^{-6} S m^{-1}), suggesting that these in-situ snow packs were likewise mature as expected (Sect. 2), and indeed agrees with the absence of consistent spatial or temporal changes in either pH or electrical conductivity throughout the survey periods. The pH-corrected zeta potential (Fig. 7b in Kulessa et al., 2012) had values around zero for the range of electrical conductivities (1–5×10^{-6} S m^{-1}) measured at Rhone Glacier and Jungfraujoch (1–5×10^{-6} S m^{-1}), and its rate of change became minimal along with those of pH and electrical conductivity (Figs. 6b and 7b in Kulessa et al., 2012). A small and invariant

zeta potential value therefore applies to the snowpacks at Rhone Glacier and Jungfraujoch. Indeed, the best fit between liquid water contents measured at Jungfraujoch with the Denoth meter and that modelled based on Eq. (3) is obtained when the zeta potential is assigned a value of $\sim -1 \times 10^{-5}$ V (Fig. 3b). The range of liquid water contents inferred from our hand tests at Rhone Glacier is also matched well by the model for all three days when this value of the zeta potential is used (Fig. 3a). Because this "best estimate" of zeta potential (-1×10^{-5} V) is small and negative, and a single zeta potential value produces an excellent fit with all of our liquid water content measurements (Fig. 3), we conclude that the self-potential method does indeed show considerable promise as a non-intrusive snow-hydrological sensor.

5 Objective 2: self-potential sensitivity to uncertainty in snow properties

We evaluate the sensitivity of predicted liquid water contents to both combined and individual parameter uncertainties. The former was achieved by running our model based on Eq. (3) numerous times for each of our four surveys (i.e. one day at Jungfraujoch and three consecutive days at Rhone Glacier); first with our best estimates as measured in-situ and inferred from Eqs. (4) and (5) and our zeta-potential considerations, and then sequentially with all possible combinations of the model, minimum and maximum values of the uncertainty range (respectively field data minus and plus uncertainty) (Fig. 3 and Supplement). These ranges were based on the uncertainties inherent in measured parameters (Sect. 3, Table 1) and the large potential uncertainty in the zeta potential, arbitrarily assigned 50 % for illustrative purposes (Sect. 4). The two latter model runs thus provide reasonable upper and lower bounds on predicted liquid water contents for comparison with our field measurements.

Despite our consideration of extreme potential error bounds, modelled uncertainties in liquid water contents are restricted to the relatively small range of $\sim$ 1–3 % at both Rhone glacier and Jungfraujoch, and absolute values remain within the pendular regime where water bodies in the pore space remain isolated At the latter site the daily

evolution of liquid water contents thus is well captured even if uncertainty is taken into account (Fig. 3b), and likewise at Rhone glacier modelled liquid water contents plus uncertainties still fall within the range of field measurements (Fig. 3a). Our inferences thus not only support Kulessa et al.'s (2012) notion that existing snow hydrological relationships are robust for modelling purposes, but also suggest that they may apply to in-situ field surveys. These inferences can also provide an explanation for the relatively large self-potential magnitudes generated by relatively low bulk discharge at Jungfraujoch (Fig. 2). Because we did not observe or infer any consistent or statistically-significant differences between Rhone glacier and Jungfraujoch in dielectric permittivity (ε), zeta potential (ζ), saturation ($S_w S_e^{-n}$), electrical conductivity (σ_w) or cross-sectional area (A), the only remaining parameter that could facilitate the observed relative difference is permeability (k). Indeed, using an average snow density of $564\,kg\,m^{-3}$, the differences in mean snow grain sizes between Rhone glacier (1.5×10^{-3} m) and Jungfraujoch (1×10^{-3} m) translate into respective permeabilities of 9.7×10^{-5} and 4.3×10^{-5} m^2. The relatively reduced permeability of Jungfraujoch's accumulation-area snow-pack therefore likely supported the presence of self-potential magnitudes that were markedly elevated relative to Rhone glacier's ablation-area snow-pack (Eq. 3). This inference emphasises the sensitivity of the self-potential method to permeability as a fundamental snow-hydrological property, along with its observed sensitivity to bulk melt water discharge and inferred sensitivity to liquid water content.

Model sensitivities to individual parameter uncertainties were evaluated by running our model separately for the maximum and minimum values considered for each individual parameter (Table 1) and subsequently differencing the outputs, whilst keeping the other parameters constant. The results cluster broadly in three categories of sensitivity, including the zeta potential (up to ~ 12 % change in liquid water content within the 50 % uncertainty range), followed by grain diameter, survey area width and snow density (~ 1–3 % change) and bulk discharge, electrical conductivity, snow depth and self-potential (< 1 % change) (Fig. 4). These three categories readily reflect our knowledge of or ability to measure in-situ the respective parameters, with surprisingly low

sensitivity to cross-sectional area (survey area width × snow depth) despite our simplistic modelling approach and significant inherent assumptions (i.e. 1–4 in Sect. 4). Self-potential magnitudes are readily measured in the field with minimum uncertainty (Fig. 4), although the strongly enhanced sensitivity to the zeta potential highlights the need for focused research to tightly constrain possible values of this parameter in in-situ snow packs.

6 Objective 3: implications for future snow hydrological research and practice

Building on Kulessa et al. (2012) fundamental theoretical and laboratory work, our study implies that the self-potential method can respectively characterize bulk meltwater fluxes in or liquid water contents of in-situ snowpacks, if independent water content or flux estimates are available. The method's ability to sense bulk meltwater fluxes in snow directly is unique because they are not readily measureable with existing techniques. The acquisition of self-potential data promises to be readily automated for snow hydrological monitoring (Kulessa et al., 2003a, b, 2012), and once a snow pack has experienced initial stages of melt, uncertainty in the snow physical and chemical properties on which self-potential magnitudes depend becomes small for measurement and modelling purposes. Four key areas of future development can be identified, including:

- the determination of absolute values of the zeta potential in in-situ snowpacks for modelling purposes;
- the experimental confirmation that the impact on self-potential magnitudes of the preferential elution of ions from and metamorphosis of freshly fallen snow is time-limited to initial stages of melt;
- the development of a rugged bespoke system for multi-dimensional self-potential monitoring in snow-hydrological research and practice;

– the experimental identification of the impact of small-scale variations in snow properties (e.g. structural inhomogeneity, anisotropy in hydraulic conductivity, micro-topography) on self-potential magnitudes;

– the stochastic assimilation of self-potential data in leading snow models such as JULES (Best et al., 2011), CROCUS (Vionnet et al., 2012) or SNOWPACK (Bartelt and Lehning, 2002; Lehning and Fierz, 2008).

We conclude that the integration of self-potential measurements into existing snow measurement and data assimilation routines shows considerable promise in supporting a reduction of uncertainty in predictive models used in operational snow forecasting.

The Supplement related to this article is available online at doi:10.5194/tcd-9-4437-2015-supplement.

Acknowledgements. This work was carried out while SST was working at VAW ETH Zurich within the Swiss National Science Foundation project; accelerated release of persistent organic pollutants (POPs) from Alpine glaciers, Research Grant 200021_130083/1 BAFU, with support of the Swiss Federal Office for the Environment (FOEN/BAFU). We would like to thank Martin Funk and VAW for hosting and supporting the work and for extensive financial support for fieldwork. Also thanks to Fabian Wolfsperger at WSL-Insititute for Snow and Avalanche Research SLF and Ludovic Baron at UNIL Université de Lausanne for providing equipment for fieldwork. Thanks to Jordan Mertes, Celia Lucas, Saskia Grindreaux, Barbara Reyes-Trüssel and Moira Thompson for invaluable help in the field.

References

Barnett, T. P., Adam, J. C., and Lettenmaier, D. P.: Potential impacts of a warming climate on water availability in snow-dominated Regions, Nature, 438, 303–309, doi:10.1038/nature04141, 2005.

Bartelt, P. and Lehning, M.: A physical snowpack model for the Swiss avalanche warning, Part I: Numerical model, Cold Reg. Sci. Technol., 35, 123–145, doi:10.1016/S0165-232X(02)00074-5, 2002.

Best, M. J., Pryor, M., Clark, D. B., Rooney, G. G., Essery, R.L. H., Ménard, C. B., Edwards, J. M., Hendry, M. A., Porson, A., Gedney, N., Mercado, L. M., Sitch, S., Blyth, E., Boucher, O., Cox, P. M., Grimmond, C. S. B., and Harding, R. J.: The Joint UK Land Environment Simulator (JULES), model description – Part 1: Energy and water fluxes, Geosci. Model Dev., 4, 677–699, doi:10.5194/gmd-4-677-2011, 2011.

Campbell, F. M. A., Nienow, P. W., and Purves, R. S.: Role of the supraglacial snowpack in mediating meltwater delivery to the glacier system as inferred from dye tracer investigations, Hydrol.Process., 20, 969–985, doi:10.1002/hyp.6115, 2006.

Colbeck, S. C., Akitaya, E., Armstrong, R., Gubler, H., Lafeuille, J., Lied, K., McClung, D., and Morris, E.: The International Classification for Seasonal Snow on the Ground, The International Commission on Snow and Ice of the International Association of Scientific Hydrology, University of Colorado, Boulder, CO, 1990.

Darnet, M., Marquis, G., and Sailhac, P.: Estimating aquifer hydraulic properties from the inversion of surface streaming potential (SP) anomalies, Geophys. Res. Lett., 30, 1679, doi:10.1029/2003GL017631, 2003.

Denoth, A.: An electronic device for long-term snow wetness recording, Ann. Glaciol., 19, 104–106, 1994.

Doherty, R., Kulessa, B., Ferguson, A. S., Larkin, M. J., Kulakov, L. A., and Kalin, R. M.: A microbial fuel cell in contaminated ground delineated by electrical self-potential and normalized induced polarization data, J. Geophys. Res., 115, G00G08, doi:10.1029/2009JG001131, 2010.

Drzymala, J., Sadowski, Z., Holysz, L., and Chibowski, E.: Ice/water interface: zeta potential, point of zero charge, and hydrophobicity, J. Colloid Interf. Sci., 200, 229–243, 1999.

Essery, R., Morin, S., Lejeune, Y., and Ménard C. B.: A comparison of 1701 snow models using observations from an alpine site, Adv. Water Resour., 55, 131–148, doi:10.1016/j.advwatres.2012.07.013, 2013.
Fierz, C., Armstrong, R. I., Durand, Y., Etchevers, P., Greene, E., McClung, D. M., Nishimura, K., Satyawali, K., and Sokratov, S. A.: The International Classification for Seasonal Snow on the Ground, IHP-VII Technical Documents in Hydrology No. 83, IACS Contribution No. 1, UNESCO-IHP, Paris, 2009.
Glen, J. W. and Paren, J. G.: The electrical properties of snow and ice, J. Glaciol., 15, 15–38, 1975.
Harper, J. T. and Bradford, J. H.: Snow stratigraphy over a uniform depositional surface: spatial variability and measurement tools, Cold Reg. Sci. Technol., 37, 289–298, doi:10.1016/S0165-232X(03)00071-5, 2003.
Kallay, N., Cop, A., Chibowski, E., and Holysz, L.: Reversible charge of ice-water interface, II: Estimation of equilibrium parameters, J. Colloid Interf. Sci., 259, 89–96, doi:10.1016/S0021-9797(02)00179-0, 2003.
Kulessa, B., Hubbard, B. P., and Brown, G.: Cross-coupled flow modelling of coincident streaming and electrochemical potentials, and application to subglacial self-potential (SP) data, J. Geophys. Res., 108, 2381, doi:10.1029/2001JB001167, 2003a.
Kulessa, B., Hubbard, B. P., and Brown, G.: Earth tide forcing of glacier drainage, Geophys. Res. Lett., 30, 11-1–11-4, doi:10.1029/2002GL015303, 2003b.
Kulessa, B., Chandler, D. C., Revil, A., and Essery, R. L. H.: Theory and numerical modelling of electrical self-potential (SP) signatures of unsaturated flow in melting snow, Water Resour. Res., 48, W09511, doi:10.1029/2012WR012048, 2012.
Lehning, M. and Fierz, C.: Assessment of snow transport in avalanche terrain, Cold Reg. Sci. Technol., 51, 240–252, doi:10.1016/j.coldregions.2007.05.012, 2007.
Livneh, B., Xia, Y., Mitchell, K. E., Ek, M. B., and Lettenmaier, D. P.: Noah LSM snow model diagnostics and enhancements, J. Hydrometeorol., 11, 721–738, doi:10.1175/2009JHM1174.1, 2010.
Mitterer, C., Heilig, A., Schweizer, J., and Eisen, O.: Upward-looking ground-penetrating radar for measuring wet-snow properties, Cold Reg. Sci. Technol., 69, 129–138, doi:10.1016/j.coldregions.2011.06.003, 2011.
Petiau, G.: Second generation of lead-lead chloride electrodes for geophysical applications, Pure Appl. Geophys., 157, 357–382, doi:10.1007/s000240050004, 2000.

Revil, A., Naudet, V., Nouzaret, J., and Pessel, M.: Principles of electrography applied to self-potential elecrokinetic sources and hydrogeological application, Water Resour. Res., 39, 1–14, doi:10.1029/2001WR000916, 2003.
Revil, A., Titov, K., Doussan, C., and Lapenna, V.: Application of the self-potential method to hydrological problems, in: Applied Hydrogeophysics, edited by: Vereecken, H., Binley, A., Cassiani, G., Revil, A., and Titov, K., Springer, the Netherlands, 255–292, 2006.
Sheffer, M. R. and Oldenburg, D. W.: Three dimensional modelling of streaming potential, Geophys. J. Int., 169, 839–848, doi:10.1111/j.1365-246X.2007.03397.x, 2007.
Shimizu, H.: Air permeability of deposited snow, Low Temp. Sci. Ser. A, 22, 1–32, 1970.
Sturm, M., Holmgren, J., and Liston, G. E.: A seasonal snow cover classification system for local to global applications, J. Climate, 8, 1261–1283, 1995.
Thompson, S. S., Kulessa, B., and Luckman, A.: Integrated electrical resistivity tomography (ERT) and self-potential (SP) techniques for assessing hydrological processes within glacial lake moraine dams, J. Glaciol., 58, 1–10, doi:10.3189/2012JoG11J235, 2012.
Vionnet, V., Brun, E., Morin, S., Boone, A., Faroux, S., Le Moigne, P., Martin, E., and Willemet, J.-M.: The detailed snowpack scheme Crocus and its implementation in SURFEX v7.2, Geosci. Model Dev., 5, 773–791, doi:10.5194/gmd-5-773-2012, 2012.
Williams, M. W., Erickson, T. A., and Petrzelka, J. L.: Visualising meltwater flow through snow at the centimetre-to-metre scale using a snow guillotine, Hydrol. Process., 24, 2098–2110, doi:10.1002/hyp.7630, 2010.

Table 1. Model input parameters and their relative maximum uncertainty and sensitivity ranges.

Measured parameter	Uncertainty range	Sensitivity values
Self-potential ψ_m (V)	$\psi_m \pm 20\,\%$	$\psi_m \pm 20\,\%$
Discharge Q ($m^3\,s^{-1}$)	$Q \pm 20\,\%$	$Q \pm 40\,\%$
Electrical conductivity of melt σ_w ($S\,m^{-1}$)	$\sigma_w \pm 5 \times 10^7$	$\sigma_w \pm 1 \times 10^6$
Zeta potential ζ (V)	$\zeta \pm 50\,\%$	10^{-3}–10^{-7}
Permeability from;		
Grain diameter d (m)	$d \pm 0.0005$	$d \pm 0.001$
Density ρ ($kg\,m^3$)	$\rho \pm 70$	$\rho \pm 140$
Cross sectional area from;		
Width w (m)	$w \pm 5$	$w \pm 10$
Depth dp (m)	dp $\pm$ 0.2	dp $\pm$ 0.4

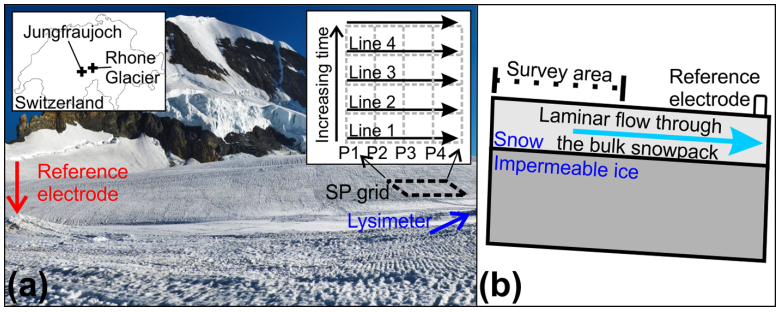

Figure 1. (a) Example survey set up. Insert left show the location of both fieldsites. Insert right illustrates the self-potential survey design; to provide each self-potential data value, a profile of 25 data points (P1, P2, etc.) was collected (Line 1, Line 2, etc.), perpendicular to assumed bulk water flow. **(b)** Schematic of the self-potential experiment developed by Kulessa et al. (2012) for the situ snowpack surveys.

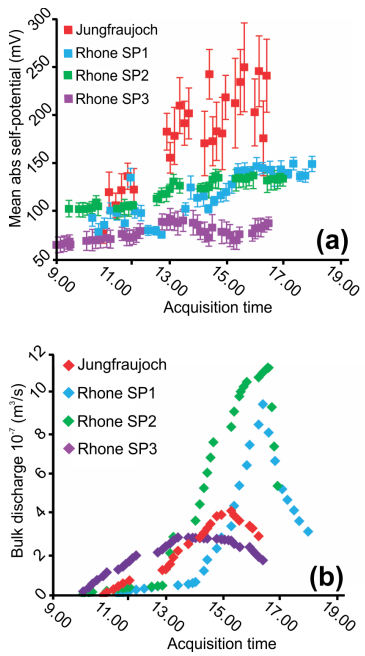

Figure 2. Time series of **(a)** bulk self-potential measurements and **(b)** bulk discharge measurements for the three Rhone Glacier surveys and the Jungfraujoch survey. Each self-potential data point represents the mean value of a profile (consisting of 25 data points); the error bars illustrates the variability over each profile. Bulk discharge was measured over each profile by the lysimeter.

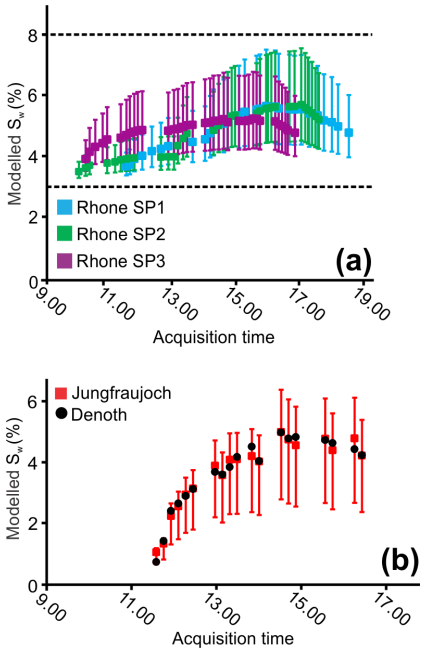

Figure 3. (a) Modelled liquid water content for each of the three self-potential surveys carried out at Rhone Glacier. The uncertainty range illustrates the minimum and maximum model results for the range of input parameters (Table 1, Supplement). All results are within the range of liquid water content (% vol) estimated by the hand tests (black dashed lines). **(b)** Model results for the self-potential survey carried out at Jungfraujoch, with the corresponding Denoth measurements.

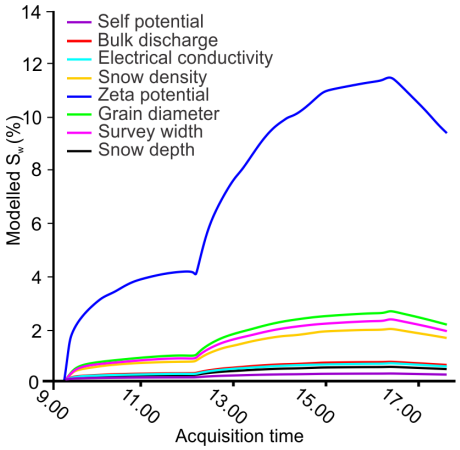

Figure 4. The difference in model results to the minimum and maximum parameter value from the uncertainty range (Table 1), highlighting the model sensitivity to each of the measured input parameter individually.